Phase identification by a novel needle-contact capacitance probe in gas-liquid two-phase flows

HUANG Shanfang[1,2,*] LU Jun[3] ZHANG Bingdong[2] WANG Dong[2]

[1]*Department of Engineering Physics, Tsinghua University, Beijing 100084, China*

[2]*State Key Laboratory of Multiphase Flow in Power Engineering, Xi'an Jiaotong University, Xi'an 710049, China*

[3]Beijing Aerospace Institute for Metrology and Measurement Technology, Beijing 100076, China

Abstract In this paper, we propose a novel probe to identify phases in any two-phase flows where one phase is conductive and the other nonconductive. We can further obtain many parameters such as void fraction, bubble velocity, and interfacial area concentration. Compared with the traditional probe, the novel probe has unique advantages that it is less dependent on water conductance or distance between the electrodes, and that the amplitude is bigger between high and low levels. Theoretical analyses showed that the measurement error became higher when water conductance decreases or distance increases, which is consistent with the theoretical analyses. Experimental results showed that the output signal kept constant with salt content of 0−5% and electrode distance of 0−30 mm in tap water. The level difference was up to 6.4 V, resulting in identifying two phases easily. Time traces of phase identification were completely consistent with the flow structures.

Key words Needle-contact capacitance probe, Phase identification, Flow structure

1 Introduction

Two-phase flows exist in industrial processes of nuclear engineering, petroleum engineering, chemical engineering, etc. Phase identification is necessary for measuring parameters of void fraction, bubble velocity, and interfacial area concentration, so as to monitor the processes, analyze the mechanism and establish related models. For local phase identification, a probe is often inserted into flow fields to contact with fluids directly. Based on physical differences of the two phases, a variety of techniques have been developed, such as optical probe[1−3], observation[4], conductance probe[5–10], etc. In terms of safety, economics and convenience, conductance probe is advantageous and has been widely used in multiphase flows in the past several decades. However, it is disadvantageous in that the accuracy is enslaved to the conductance of the conductive phase or the distance between the electrodes. Large measurement errors can occur when the conductance varies too much in a flow process. To avoid the disturbance of conductance or distance, an intrusive capacitance probe, namely single-wire capacitance probe, was used to measure water layer height[11−13], and identify flow patterns[14] in air-water or oil-water two-phase flows. The measurement results were stable despite big changes in salinity (or conductance) of the water.

In this paper, we propose a novel probe, namely needle-contact capacitance probe, to identify local phases in two-phase flows without the conductance dependence. The working principle is deduced and validated, and simple applications are given.

2 Working principle of the probe

Fig.1 shows a sketch of the needle-contact capacitance probe. When the fluid between the electrodes is

Support by the National Natural Science Foundation of China (No. 51006068).

* Corresponding author. *E-mail address:* sfhuang@mail.tsinghua.edu.cn

Received date: 2010-09-18

conductive, e.g. water, the circuit is close and a certain value can be read on the capacitance meter, whereas if the fluid is not conductive, the circuit is open, hence no output. In two-phase flows, e.g. air-water flow, conductive and nonconductive phases alternately pass the gap between the electrodes, the circuit is accordingly close or open, and this allows identification of the two phases.

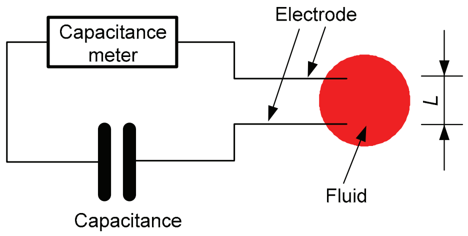

Fig.1 Sketch of needle-contact capacitance probe.

The circuit can be analyzed as follows. Since its frequency is low enough to be neglected, the circuit has an equivalent circuit as shown in Fig.2(a), where the constant capacitance C_0, water capacitance C_w, contact resistance r, and water resistance R_w are connected in series. If everywhere of the circuit is well connected, we have

$$R_W >> r,\ C_w >> C_0. \quad (1)$$

By neglecting r and C_w, the circuit is simplified to the circuit of Fig. 2 (b), with a time constant of $\tau = R_w C_0$.

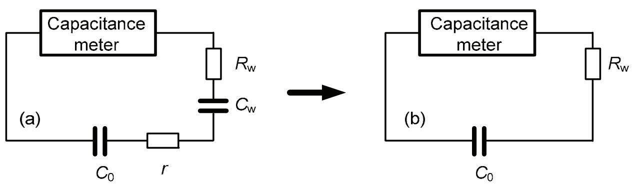

Fig.2 Equivalent circuit of the probe.

Therefore, we can see that the circuit performance is mainly determined by two factors, the constant capacitance and conductivity of the fluid. A capacitance should be as big as possible to minimize the influence of scattered capacitance, whereas, it should be as small as possible to maximize the detection speed. As a compromise, we chose a capacitance of 50 pF. Five kinds of fluid were chosen, too: deionized water, distilled water, tap water, mineralized water, and industrial waste water. With a hypothesized cubic water drop of 1 mm^3 between the two electrodes, the resistance is equal to conductance in number. Table 1 shows the estimated time constant τ.

Table 1 Time constant of a needle-contact probe in different flows.

Kinds of water	Conductance / Ω·cm	Resistance / Ω	Time constant RC / s
Deionized water	10^7	10^7	5×10^{-04}
Distilled water	10^6	10^6	5×10^{-05}
Natural water	10^4	10^4	5×10^{-07}
Mineralized water	10^3	10^3	5×10^{-08}
Industrial waste water	10^2	10^2	5×10^{-09}

In practical applications of two-phase flow, the performance of a probe is determined by not only the circuit itself, but the flow conditions, namely interfacial velocity and size of discrete phase. The probe's ability to detect a bubble passing the probe varies with bubble velocity. As an example, the t_f/τ ratios, where t_f is the time for a 1-mm bubble to pass the probe, at velocities of 0.01, 0.1, 1 and 10 m/s, are shown in Fig. 3. The t_f/τ ratio reflects the probe performance, which depends very much on the flow conditions. The measurement accuracy increases with the t_f/τ ratio. Since the time ratio is far below 1 for some cases, e.g. deionized water, the detection frequency is very low, so that the probe loses the detection ability completely. On the other hand, the time ratio is much larger than 1 with the mineralized water and industrial waste water, hence a much better probe performance. Generally, the detection ability increases with the bubble size, but decreases with increasing velocity and fluid resistance.

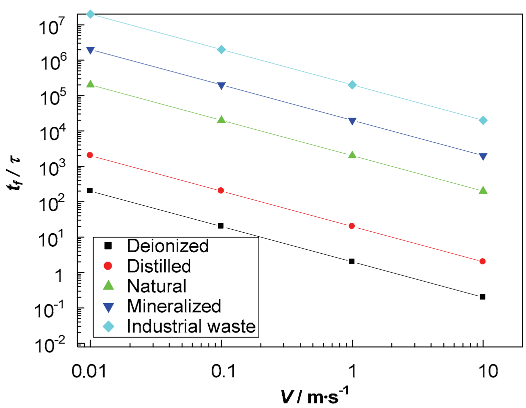

Fig.3 Ratio of passing time to time constant, t_f/τ, for a 1-mm bubble in different fluids.

The effective capacitance from the measurement circuit is determined by

$$C_e=C/[1+(\omega R C)^2] \quad (2)$$

where ω is the detection frequency of the circuit. Therefore, C_e is always smaller than the true value C. A maximum C_e is achieved by minimizing ωRC. In some cases, e.g. deionized water, the detection frequency must be very low to keep C_e above a certain value.

In a practical application, parameters related to the probe itself are generally constant, such as water conductance, distance between the two electrodes, and frequency, so the performance is determined by flow conditions. For example, shape, size, and velocity of water film over the electrodes' surface vary as the two phases pass the probe alternately, and these change the resistance R in Fig.2. Therefore, we should focus on the effect of flow conditions.

3 Experimental

To validate the working principle of the proposed probe, static experiments were carried out at different water salinities and electrode-gap widths. Two electrodes, made of Φ1 mm stainless steel wire, with the gap width of up to 30 mm, were inserted into tap water for 10 mm to ensure that the electrodes contacted with water fully. The water salinity was increased to up to 5% by adding salt into water continually. The constant capacitance was 80 pF, measured by RCL impedance instrument (PM6304, Fluke Corp., USA).

As shown in Fig.4, the measured capacitance C_m kept the same (Fig. 4a) at salinities of $\leq$ 5%, and so did the output capacitance (Fig. 4b) throughout the gap widths. Therefore, the needle-contact capacitance probe is independent of the water salinity or the electrode gap width.

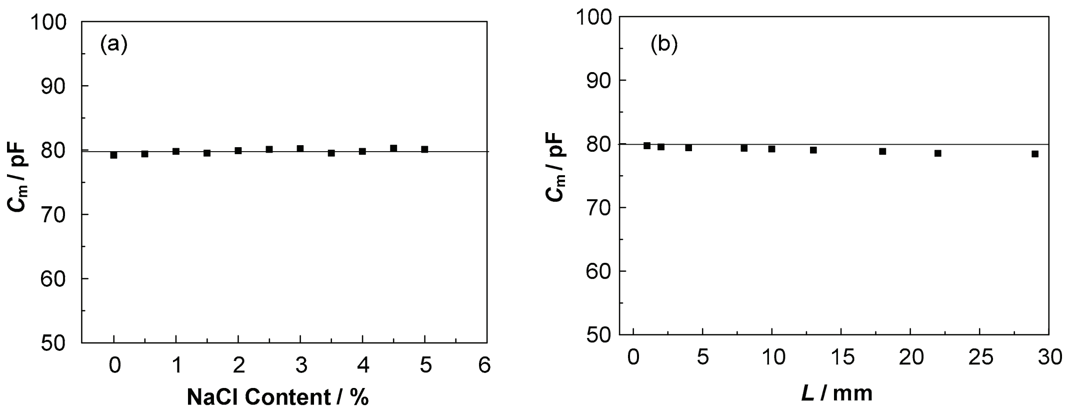

Fig.4 Effect of (a) salinity and (b) electrode gap width on probe performances.

A horizontal test section (Fig.5), made of transparent Plexiglas pipe of D_{inner} = 40 mm, in length of L = 8 m (L/D = 200) from the front end to the electrode tip, was long enough to ensure full development of air-water mixture before entering the test probe. The constant capacitance was 100 pF. The needle-contact capacitance probe was made of Φ0.2 mm nichrome alloy wire, which was inserted into a Φ1.5 mm stainless steel tube of inner diameter. The alloy wire and the stainless steel tube, insulated from each other by epoxy resin, acted as two electrodes of the probe. The probe was vertically inserted into the Plexiglas pipe with a horizontal bending length of 5 mm, which was 17 mm to the upper wall of the pipe. Only the wire tip in length of 0.5 mm was used to identify the fluids passing the tip, and the tube was just a support to the wire.

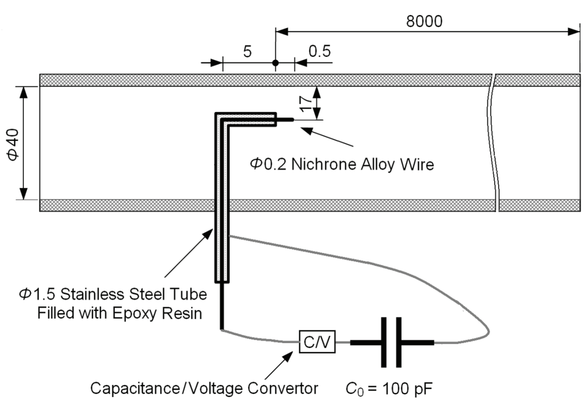

Fig.5 Structure of test section.

The circuit for converting capacitance into voltage (C/V) is similar to that in Refs.[12–13]. According to the C/V circuit calibration (Fig.6), the voltage curve can be divided into three parts. When the input capacitance is less than 50 pF (Part A), the output voltage is 0 V. When it is over 100 pF (Part C), the output voltage is at the maximum (6.4 V). From 50 pF to 100 pF, the output voltage rises monotonously, with decreasing slopes towards zero at last. In dynamic experiments, if the conductive phase, water, passes the probe tip, the circuit is closed and the output voltage reaches the maximum 6.4 V (high level), while the output is 0 V (low level) when the air phase passes the tip. Theoretically, we can thus obtain square waves against time.

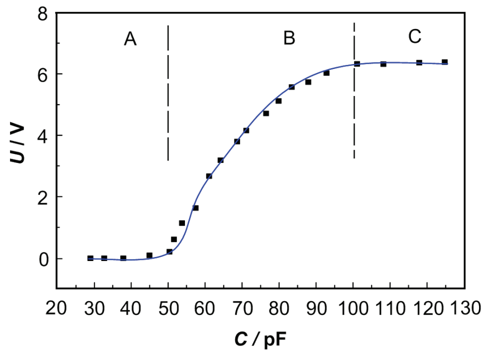

Fig.6 Output signals of capacitance-to-voltage circuit (C/V).

However, the practical time traces are not normatively binary when the interface passing the tip. It is necessary to process the practical time traces to obtain normative binary square wave for further analysis. A conventional method is to set a threshold voltage $U_{\text{threshold}}$ according to the calibration results by e.g. a high-speed video system. When the output voltage is over $U_{\text{threshold}}$, the processed signal $P(t)$ corresponds to the high level. Otherwise, it corresponds to the low level. The processing method is summarized as follows:

$$P(t) = \begin{cases} 1 & U>U_{\text{threshold}}\text{, when the tip is in water} \\ 0 & U<U_{\text{threshold}}\text{, when the tip is in air} \end{cases} \qquad (3)$$

We set $U_{\text{threshold}}$ =3.2V in this study, according to the high-speed video results.

Dynamic experiments, for studying effects of the probe structure, interface shape and velocity, were carried out in the multiphase flow loop, and the effects related to flow pattern, e.g. interfacial velocity and shape, were to analyzed.

The superficial velocities of air and water were adjusted to obtain the needed flow pattern according to flow pattern map in air-water two-phase flows. Special attentions were paid to calculate air superficial velocity. The air velocity was calculated with parameters obtained *in-situ* in the test section. The flow pattern was intermittent flow including plug and slug flows, where there are many kinds of bubbles of different shapes and sizes.

When the flow was steady, different working conditions of pressure, temperature, flow rates etc. were recorded. Then the circuit measurements were started to record time traces at the time period of 10 s and sampling frequency of 1000 Hz.

It is necessary to transform the obtained signals into square waves according to Eq.(3), so as to estimate the measurement accuracy and calculate parameters of the flow processes.

4 Results and discussion

Fig.7 shows the experimental result in plug flow, where the liquid slug and the gas bubble passed the probe alternatively. The superficial velocities of gas and liquid were 0.38 m/s and 0.78 m/s, respectively. The interfacial velocity was small with a big curvature radius, so the working condition of the probe is similar to that in the static experiments. From the time trace in Fig.7(a), there should be a water droplet connecting the SS tube and the probe tip, resulting in a low level of 0.8 V instead of 0 V. The shape of the time trace is almost the same as the normative square wave (Fig.7b) except the bubble head.

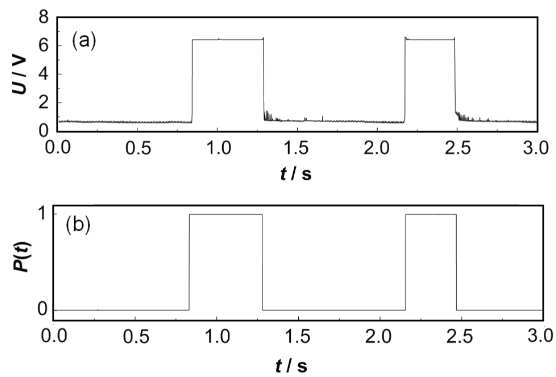

Fig.7 Output signals (a) of the capacitance probe in plug flow (V_{sg} = 0.38 m/s, V_{sl} = 0.73 m/s), and the processed signals (b).

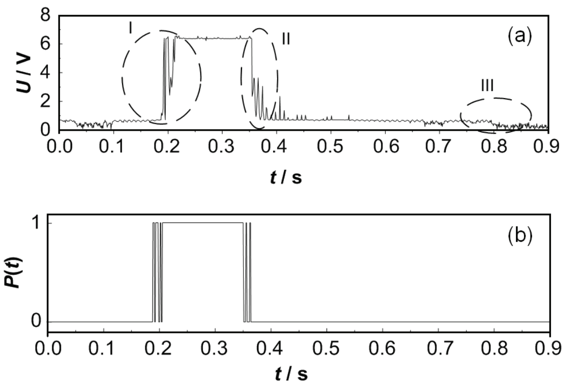

Fig.8 Output signals (a) of the local capacitance probe in slug flow (V_{sg} = 1.55 m/s, V_{sl} = 0.36 m/s), and the processed signals (b).

The time trace in slug flow (Fig.8), at superficial velocities of gas and liquid of 1.55 m/s and 0.36 m/s, respectively, is much more complicated than that in the plug flow. Slug flow is of high velocity, with many bubbles of different sizes and shapes entrained in the liquid. To show the time trace clearly, Fig.6 gives just one slug unit within 0.9 s. The time trace has three typical parts: slug head, slug tail and long bubble. As a whole, the output signals of the circuit can reflect roughly the structure of the slug body, but small bubbles entrained in the slug were obviously omitted to different extents.

This novel method to identify phases in two-phase flows can be improved in measurement accuracy and spatial resolutions in following ways.

1) To improve the probe resolution, the structure and the size shall be optimized by several approaches, including coniform shape of the tip, insulation to the probe except the very tip, and high dewetting ability.

2) Flow patterns, related to bubble size and velocity, are crucial to the probe performance. The detection ability increases with bubble size, but decreases with increasing bubble velocity.

3) A threshold value has been used to obtain square wave signals, but this brings errors. A better way is to process the data according to features of the output signals.

Besides common influential factors to performances of conductance and capacitance probes, there are some unique factors for capacitance probe, e.g. electrode placement, and the circuit. The electrodes may be placed separately to reduce the hinderance, with one electrode in the flow and the other fixed to the pipe. The circuit can be improved by optimizing the parameters.

Efforts shall be made in obtaining $U_{\text{threshold}}$, optimizing the flow structure, measuring the errors quantitatively in different two-phase flows, and obtaining more parameters, including void fraction, interfacial velocity, bubble size, and interfacial area concentration.

5 Conclusions

This study proposed a method to identify phases in any two-phase flows with one conductive phase and the other nonconductive. The detection ability increases as bubble size increasing, velocity decreasing, or resistance of conductive phase decreasing. The output signals were independent of salt content of 0–5%, or distance between the two electrodes of 0–30 mm. The output signals were qualitatively consistent with the flow structures of intermittent flows in air-water two-phase flows.

References

1 Fordham E J, Holmes A, Ramos R T, *et al*, Meas Sci Technol, 1999, **10**: 1329 – 37.

2 Fordham E J, Simonian S, Ramos R T, *et al*, Meas Sci Technol, 1999, **10**: 1338 – 46.

3 Fordham E J, Ramos R T, Holmes A, *et al* Meas Sci Technol, 1999, **10**: 1347 – 52.

4 Gopal M, Jepson W P. Int J Multiphase Flow, 1997, **23**: 945–65.

5 Angeli P, Hewitt G F. Int J Multiphase Flow, 2000, **26**: 1117–40.

6 Hibiki T, Ho Lee T, Young Lee J I. Chem Eng Sci, 2006, **61**: 7979–90.

7 Hazuku T, Takamasa T, Hibiki T. Int J Heat Mass Transfer, 2007, **50**: 2986–95.

8 Zheng D H, Che D F. Int J Multiphase Flow, 2006, **32**:1191–1218.

9 Prasser H M, Bottger A, Zschau J. Flow Meas Instru, 1998, **9**: 111–119.

10 Prasser H M, Misawa M, Tiseanu I. Flow Meas Instru, 2005, **16**:73–83.

11 Fagundes Netto J R, Fabre J, Peresson L. Int J Multiphase Flow, 1999, **25**: 1129–60.

12 Huang S F, Zhang X G, Wang D, *et al.* Meas Sci Technol, 2007, **18**: 3784–94.

13 Huang S F, Zhang X G, Wang D *et al.* Int J Multiphase Flow, 2008, **34**:809–18.

14 Huang S F, Zhang B D, Lu J *et al.* Nucl Sci Techni, 2010, **21**: 246–250.